Universidade de Aveiro

Departamento de Engenharia de Materiais e Cerâmica
(DEMaC)

Ano 2018/2019

Helena Beatriz Gomes Cardoso

Desenvolvimento de um biossensor descartável para a deteção do antigene 15-3 do cancro da mama

Development of disposable biosensor for the detection of breast cancer antigen 15-3

Universidade de Aveiro

Ano 2018/2019

Departamento de Engenharia de Materiais e Cerâmica (DEMaC)

Helena Beatriz Gomes Cardoso

Development of disposable biosensor for the detection of breast cancer antigen 15-3

Dissertação apresentada à Universidade de Aveiro para cumprimento dos requisitos necessários à obtenção do grau de Mestre em Materiais e Dispositivos Biomédicos, realizada sob a orientação científica da Doutora Teresa Rocha-Santos, Investigadora Principal do Departamento de Química e CESAM da Universidade de Aveiro e do Doutor João Pinto da Costa, investigador Auxiliar do Departamento de Química e CESAM da Universidade de Aveiro

Aos meus pais, namorado e amigos por toda a paciência e apoio.

o júri

presidente

Prof. Doutor João André da Costa Tedim
Professor Auxiliar em Regime Laboral da Universidade de Aveiro

Doutora Patrícia Sofia Matos dos Santos
Investigadora Júnior da Universidade de Aveiro

Doutor João Pinto da Costa
Investigador Doutorado da Universidade de Aveiro

agradecimentos

Ao Professora Doutora Teresa Rocha Santos pela orientação prestada, pela disponibilidade e apoio que demonstraram.

Ao Professor Doutor João Pinto da Costa por todo o tempo de trabalho que me dedicou e me ajudar sempre que necessário.

Aos colegas de laboratório agradeço toda a simpatia e apoio.

Aos meus pais pela paciência, presença e carinho. Obrigada
por todo este investimento e apoio incondicional e por me deixarem sonhar.

Ao meu namorado por ter estado sempre ao meu lado, pelas noites em claro, pela paciência, pelo sorriso e por a motivação para concluir esta etapa.

A todos os amigos que de uma forma direta ou indireta, auxiliaram na elaboração deste trabalho, pela paciência e alegria que prestaram em momentos menos fáceis.

palavras-chave

biosensor, cancro da mama, grafeno, ELISA, transistores de efeito de campo.

resumo

Este trabalho descreve o desenvolvimento de biossensores eletroquímicos com grafeno, para a deteção da proteína CA15-3, um reconhecido marcador tumoral do cancro da mama, utilizando transístores de efeito de campo com grafeno (Gr-FET), funcionalizados com um anticorpo específico para esta proteína. O modelo de calibração permitiu obter um coeficiente de correlação de 0.9959 e um limite de deteção de 0.07 U mL^{-1}. Os valores de recuperação obtidos demonstram a sua adequação para a quantificação da proteína CA15-3 em soluções padrão. O método de ELISA foi também utilizado como método de comparação para validação do biossensor. Adicionalmente, testou-se a exequibilidade de utilização do biossensor desenvolvido para a deteção e quantificação deste marcador em amostras de saliva, visando o desenvolvimento de uma tecnologia de baixo custo, descartável e rápida que permita uma quantificação recorrendo a métodos não invasivos, ilustrando o potencial deste método no diagnóstico de uma doença altamente prevalente.

keywords biosensor, breats cancer, graphene, ELISA, field effect transistors.

abstract This work describes the development of graphene electrochemical biosensors for the detection of CA15-3 protein, a recognized breast cancer tumor marker, using graphene-based field effect transistors (Gr-FET) functionalized with a specific antibody for this protein. The calibration model provided a correlation coefficient of 0.9959 and a detection limit of de 0.07 U mL^{-1}. The recovery values obtained demonstrate its suitability for the quantification of CA15-3 protein in standard solutions. The ELISA method was also used as a comparison method for biosensor validation. Additionally, the feasibility of using the biosensor developed for detection and quantification of this marker in saliva samples was tested, aiming at the development of a low cost, disposable and fast technology that allows quantification using non-invasive methods, illustrating the potential of this method in the diagnosis of a highly prevalent disease.

Índex

List of Figures

List of Tables

List of abbreviations

CA 15-3 – Cancer antigen

CV- Cyclic voltammetry

CV – Coefficient of variation

DPV - Differential pulse voltammetry

EIS - Electrochemical impedance spectroscopy

ELISA – Enzyme linked immunosorbent assay

FRET- Fluorescence resonance energy transfer

FET – Field-effect transistors

LOD – Limit of detection

PBS – Phosphate buffer solution

POC – Point-of-care

SWV - Square wave voltammetry.

UV-Vis – Ultraviolet-Visible

U mL^{-1} – Unity for milometer

1. Objectives

The main objective of this work was to develop, apply, and validate an electrochemical biosensor with a field effect transistor (FET) configuration and based on graphene as the transduction component, for the detection and quantification of the Carcinoma Antigen 15-3, a recognized tumor marker for multiple types of cancer, and, most notably, breast cancer.

Graphene is a nanomaterial that can be applied as the transduction component in biosensors, given its large surface area and excellent electrical conductivity, rendering this material very sensitive. When a constant voltage current is applied to the gate electrode, it crosses graphene, causing changes in the current intensity, owing to the modifications caused by this current on the surface of grapheme. These modifications can stem from either the adsorption of the specific antibody used or by the subsequent linkage to the antigen, in this case, CA 15-3.

Furthermore, within the context of this work, the use of the developed biosensor for the quantification of the antigen in saliva samples was explored, by directly assessing the presence of CA 15-3 in this bodily fluid.

In order to achieve the main objective of this work, the following tasks were carried out:

- Evaluation of the graphene dispersion in an aqueous surfactant, assessed using UV-Vis spectroscopy;
- Electrical characterization of the Gr-FET based on the variation of the measured current with applied voltage;
- Study of the analytical performance of Gr-FET for CA 15-3 detection;
- Validation of results by comparison with ELISA and;
- Assessment of the suitability of the application of the developed FET for the detection and quantification of CA 15-3 in saliva.

2. Introduction

Cancer is defined by the uncontrolled growing and spread of abnormal cells[1]. Breast cancer, more specifically, has been reported as the most common causes of death in female patients, with an estimated 1.1 new million cases each year[2]. Owing to the severe morbidity and disability caused by this specific type of cancer, early stage detection, treatment and subsequent monitoring leads not only to more effective treatments, but to lower probabilities of recurrence as well. Currently, diagnosis techniques mostly consist of mammography, biopsy, sonography, and thermography, which can detect between 80 to 90% of the cases[3]. However, these methodologies are of limited sensitivity, show high numbers of false-positive results and may lead to accumulated radiation in the body. Additionally, these are approaches that are frequently used once there are some other associated symptoms, thus sometimes resulting in late diagnoses.

Determining molecular abnormalities in breast cancer becomes, therefore, an important strategy for early detection, prognosis, treatment selection, as well as treatment monitoring. Products cellularly secreted as a result of the presence of cancerous cells may have emerged as powerful tools for cancer screening, and these, termed "biomarkers", have been defined as "(…) anything present in or produced by cancer cells or other cells of the body in response to cancer or certain benign (noncancerous) conditions that provides information about a cancer, such as how aggressive it is, whether it can be treated with a targeted therapy, or whether it is responding to treatment"[4]. Among these, different secreted products derived from the mucin-1 glycoprotein, depicted in Figure 1, are considered circulating markers, used in diagnostic in patients with breast cancer, including CA 15-3[5]. In clinical practice, the precise measurement of the levels of these markers in bodily fluids can provide key information on the tumor's response to treatment and its biological behavior during disease and treatment progress and monitoring.

Given the clinical relevance of these markers, different strategies have been developed to accurately quantify the levels of CA 15-3 and different studies have highlighted that such measurements could lead to a highly reliable predictability of treatment response, as well as disease outcome[6,7]. This protein is also present in saliva and its correlation with the presence of CA 15-3 in serum has been previously established[8]. It is therefore possible to postulate that saliva could be used as a sampling

fluid for the measurement of this biomarker, thus potentially eliminating the need of invasive procedures, and simultaneously allowing for an accurate evaluation of the health status of individuals using a disposable device.

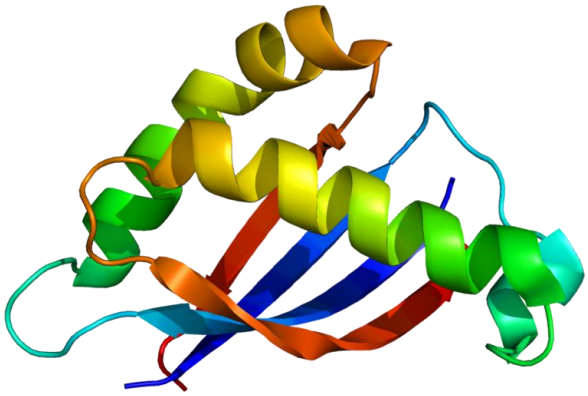

Figure 1 - Structure of the MUC1 protein. MUC1 displays extensive O-linked glycosylation of the extracellular domain. These proteins line the surface of epithelial cells in multiple organs, including the stomach and intestines, the lungs and eyes. Overexpression of MUC1 is often associated with cancer, namely, breast and lung cancers[9]*. The normal concentration in a healthy human is approximately 30 U mL*$^{-1}$*, while in subjects with cancer, this value is typically 100 U mL*$^{-1}$ [10]*Available under CC BY-SA 3.0.*

Techniques used for the quantification of CA 15-3 include enzyme linked immnusorbent (ELISA), radioimmunoassay (RIA) and immunohistochesmitry (IHC) assays. Nonetheless, such methodologies are onerous, and may exhibit false positive or false negative results[11]. Nonetheless, these are demonstrably established techniques, widely accepted and used within clinical settings, but that do not obstruct in any way the development of new, innovative, sensitive and consistent methodologies aimed at the rapid and reliable monitoring of different samples, allowing for early diagnosis and effective treatmens[1]. In fact, a fast and accurate clinical response is essential and point-of-care (POC) devices, i.e., devices that allow for medical diagnostic testing at or near the point of care, could contribute towards this goal owing to their reduced cost, fast and easy analysis and readily availble results on which health professionals can depend upon and devise clinical therapies, when needed[12]. POC devices are small, robust, fast and a multi-platform analysis and have a huge advantage against the most usual methods of

diagnosis, which, commonly, take place in more advanced stages of cancer[12]. Biomarkers are therefore the ideal analytes to be analyzed and quantified using POC devices[12].

A chemical sensor is a device that transforms chemical information from the sample in an analytical signal that can be read[13]. The sensor is typically composed of two elements, the recognition component and a physical transducer. The transducer is an electronic device that converts the interaction between the analyte and the recognition element in a measurable signal. The signal that is obtained may be electrical or optical and, then, is converted through hardware and software to a readout[13]. A sensor classified based on the transducer can be electrochemical, optical, magnetic or piezoelectric[13]. A biosensor, in turn, is a sensor in which the recognition element is a biological one[13], or, as defined by the International Union of Pure and Applied Chemistry (IUPAC), a biosensor is an "integrated receptor–transducer device, which is able to provide selective quantitative or semi-quantitative analytical information using a biological recognition element"[14]. This element may be a protein, a gene, an enzyme or other macromolecules, as an antibody or a cell receptor, polynucleotide, or micro RNA's[11]. A (bio)sensor can be classified as electrochemical (including amperometric, conductometric, impedance and potentiometric), optical (including fiber optic and surface-plasmon resonance), magnetic field and piezoelectric. Figure 2 summarizes the four transducer types and some examples of detection principles.

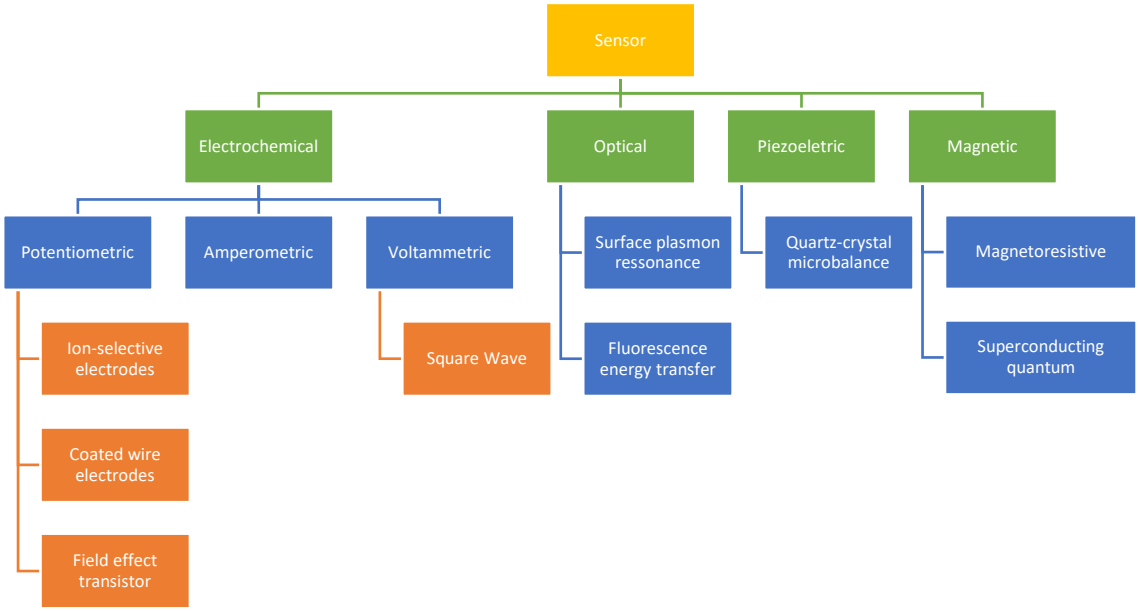

Figure 2 - Four types of transducer used in sensor and some examples of detection principles for each transducer type.

2.1 Electrochemical biosensors

Electrochemical biosensors are some of the most commonly used types of biosensors. These provide practicality, sensitivity, and fast response, and allow integration with labs-on-chips (LOCs) to obtain excellent POC analytical platforms[15]. These sensors transform biochemical information, such as analyte concentrations, into an analytically useful signal, more precisely, amperometric signals[16]. In general, the biochemical reactions, between the target molecule and the recognition element, occur on the surface of the working electrode, followed by the electrochemical readout in the transducer[17]. The device quantifies and detects the analyte through electrochemical principles such as voltammetry, amperometry, potentiometry, electrochemiluminescence (ECL), field effect transistor and electrochemical impedance. Consequently, the devices are classified by the working principle as amperometric, potentiometric, voltammetric, chemiresistive, capacitive and field effect transistor (FET), as is shown in Figure 2[12]. The latter, FET, is a device that has a solid-state with high-input impedance and low-output impedance, and monitors the charge distribution on the ion-sensing membrane[18]. It also allows interaction of the biomolecules with the transistor resulting in a redistribution of charge leading to a change in the conductivity. Consequently, very minute changes in concentrations of a specific analyte result in measurable, quantifiable current variations, which can be accurately determined[19].

2.2 Graphene as a transduction element

Graphene is a form of carbon that presents itself as a single layer of atoms in a two-dimensional hexagonal lattice, providing a high specific surface area. It shows a unique set of properties, including high conductivity of heat and electricity, and, in proportion to its thickness, it is about 100 times stronger than the strongest steel [20]. Additionally, grapheme exhibits rapid electron transport, high surface-to-volume ratio and biocompatibility due to the graphene selectivity and sensitivity to the analyte[20,21]. Due to the intrinsically exceptional charge transport, a low charge-transfer resistance, a broad electrochemical window, high mobility of charge carriers, high electron transfer rate and ability to quench fluorescence, graphene is considered very attractive for electronic applications and for sensors[21], namely, FET. The high surface-to-volume ratio allows the

enhancing of the read-out thought signal amplification. Graphene has their carbon atoms arranged in a honeycomb lattice in the two energy bands, the valence band (VB) that is completely full and the conductance band (CB) that is empty[20]. This allows the mobility of the electrons between the holes created between the bands.

Also, the unusual structure of graphene makes it more advantageous in relation to other carbon materials, such as carbon nanotubes, because of its tunable optical properties, high planar surface, mechanical strength, electron-hole symmetry and internal degrees of freedom[22], making it an exceptional transduction element in sensors and biosensors.

2.3 Antibodies as recognition elements

Antibodies are amongst the most suitable elements of biorecognition, as evidenced in Table 1. These molecules, produced by B lymphocytes and that constitute an essential part of the defense mechanisms of the immune system, display very high specificity and affinity towards specific antigens, or targeted substances, rendering them highly suited for the detection and quantification of their respective antigens[23]. On biosensors, immobilization of antibodies can be achieved through non-covalent immobilization, covalent immobilization or affinity-based immobilization.

In covalent immobilization, surface modification is necessary in order to form reactive groups (hydroxy, thiol, carboxy and amino groups) on the surface and, subsequently, the immobilization of the antibody. This immobilization helps the long-term storage and reusability of immunosensors, but requires additional steps and frequently leads to partial denaturation, which can affect the sensitivity of the biosensors. Affinity-based immobilization, proteins with a high affinity and binding specificity with specific regions on the antibody are used, helping the immobilization of the antibody in the surface of the sensor[24]. It is, however, costly and time consuming. In non-covalent immobilization, the antibody is adsorbed via electrostatic or ionic bonds, hydrophobic interactions and van der Waals forces. Fast, cheap and simple, the major drawback is the limited reusability of the manufactured biosensors, given the potential for loss during washing steps[25].

In Table 1, different types of biosensors developed for the detection of breast cancer antigen 15-3 are described, taking in consideration the detection limit and detection range. As noted in Table 1, the majority of the developed biosensors is based on the electrochemical transduction principle and use anti-CA 15-3 as bio-recognition element.

Table 1- Biosensors for the detection of breast cancer antigen 15-3

Transduction Principle	Transduction method	Element of Biorecognition	Molecule used on the biorecognition	Detection Limit	Linear range	Fluid	Reference
Electrochemical	CV	Enzyme	Glucose oxidase	0.04 U/mL	0.1 to 160.0 U mL^{-1}	Serum	[26]
Electrochemical	CV	Antibody	Anti-CA 15-3	0.012 U/mL	0.1 to 20.0 U mL^{-1}	Serum	[27]
Electrochemical	Voltammetry	Antibody	Anti-CA 15-3	5.0 U/mL	0.5 to 1.0 µg mL^{-1}	Solution	[28]
Electrochemical	EIS DPV	Antibody	Anti-CA 15-3	0.3 U/mL	1.0 to 150.0 U mL^{-1}	Serum	[29]
Electrochemical	CV EIS	Antibody	Biotinylated anti-CA 15-3	15 x 10^6 U/mL	15.0 x 10^6 to 50.0 x 10^6 U mL^{-1}	Serum	[30]
Electrochemical	CV DPV	Antibody	Anti-CA 15-3	0.02 U/mL	0.05 to 20.0 U mL^{-1}	Solution	[31]

Electrochemical	CV SWV	Antibody	Anti-CA 15-3	0,011 U/mL	0.3 to 1.0 U mL^{-1} and 2.0 to 250.0 U mL^{-1}	Serum	[32]
Electrochemical	CV DPV EIS	Antibody	Anti-CA 15-3	0,10 U/mL	0,10 to 100 U mL^{-1}	Serum	[33]
Piezoelectric	QCM	Antibody	Anti-CA 15-3	----------	0,5 to 26 U mL^{-1}	Solution	[34]
Optical	FRET	Antibody	Anti- CA 15-3	0.9 µU/mL	0.163 to 5.0 mU mL^{-1}	Serum	[35]

In a FET, the graphene acts like a conducting channel between two metals, where the current is carried, due to the rapid response of variations of gate-source voltage. When used for the detection of CA 15-3, the graphene is functionalized with anti-CA 15-3 antibodies. When CA 15-3 binds to the antibody, it causes a change in the potential on the surface of the graphene FET that leads to a change in the electrical conductivity. The detection is possible due to a change in the charged molecules and ions making possible a response signal at low concentrations of the target molecules[21].

3. Methodology

3.1 Microfabrication of field effect transistors

The FET device was microfabricated in a series of 3 silicon wafer (Figure 3 (a)) and the final configuration was based on interdigitated electrodes of 1.5µm of width and 1000µm in length. The microfabrication process involved the following steps:

1. Passivation of a wafer with SiO_2, with 400 nm-thick, through plasma and enhancing the chemical vapor deposition;

2. Deposition of Ti, 10 nm-thick, followed by deposition of Au, 100 nm-thick, in the substrate of Si/SiO_2 through physical vapor deposition by sputtering;

3. Source definition and drain metal electrodes placement through optical lithography using a 1.5 µm-thick photoresist layer coated in a standard spin coating system;

4. To remove undesired zones, ion milling of Ti/Au films was used;

5. To define the back-gate electrode with definition of a penning in the resist, 500 nm of SiO_2 were removed;

6. Deposition of Cr, 50 nm-thick, followed by deposition of Au, 100 nm-thick films through ion beam deposition right after the ion beam etching, thus avoiding a vacuum break;

7. Through lift-off, the wafer was immersed in a microchip solution at 65ºC to remove the photoresist and the Cr/Au films.

Then, the wafers were cleaned with isopropanol and distilled water and dried with N_2. After these steps, the silicon wafer was diced in order to promote individualized FET with an area of approximately 3x2 mm^2. Each individualized FET was mounted into a printed circuit board (PCB), fixed and wire bonded with Al wires (25 µm Ø) and protected with a silicone gel[36,37]. This also allowed for the inclusion of an open chamber with approximately ~1 mm Ø to be used in the sensing experiments (Figure 3 (b)). Finally, the

FET surface was washed with acetone and 1-propanol, then rinsed twice with distilled water and finally dried under N_2 flow.

3.2 Configuration of field effect transistor

FET device is formed by two *p*-type silicon wafers passivated with an insulating layer of SiO_2. A thick Cr/Au film (gate) is deposited in a layer as a back-gate configuration. It is followed by a thin layer of Au with a thick adhesion layer of Ti underneath, the source and the drain, as evidenced in the schematic view depicted in Figure 3 (c). The back-gate configuration allows the contact of the graphene with the sample, facilitating the reading and measurement of the signal in the presence of an analyte[38]. This electrical configuration between the source, drain and gate contacts is typical in a FET providing an excellent performance, such low limit of detection and high sensitivity. When a current is applied, it flows through the graphene channel and travels between the source and the drain contacts[38]. The current depends on the voltage applied and the resistance of the graphene and it is modulated by the gate contact.

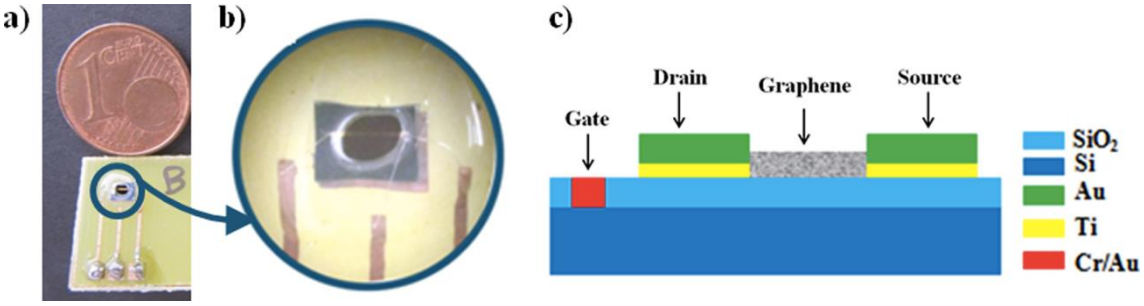

Figure 3 - a) Photograph of a part of a PCB with one individualized FET; b) zoom-image of the silicone chamber where the sensing experiments are performed; and c) schematic view of a FET with graphene. Reprinted with permission from Elsevier from J. Antunes et al. / Microchemical Journal 138 (2018) 465-471[37].

3.3 Electrical characterization of field effect transistors

The electrical measurements were made using a semiconductor parameter analyzer (*Agilent 4155C, Japan*), linked to a closed test fixture (*Agilent 16442A, Japan*)

where the device was positioned as described: in the test fixture, the drain, gate, and source of each Gr-FET were connected to their respective terminals to provide electrical circuit for sensing measurements, as seen in Figure 4. This step was performed in a room under controlled temperature of 25ºC.

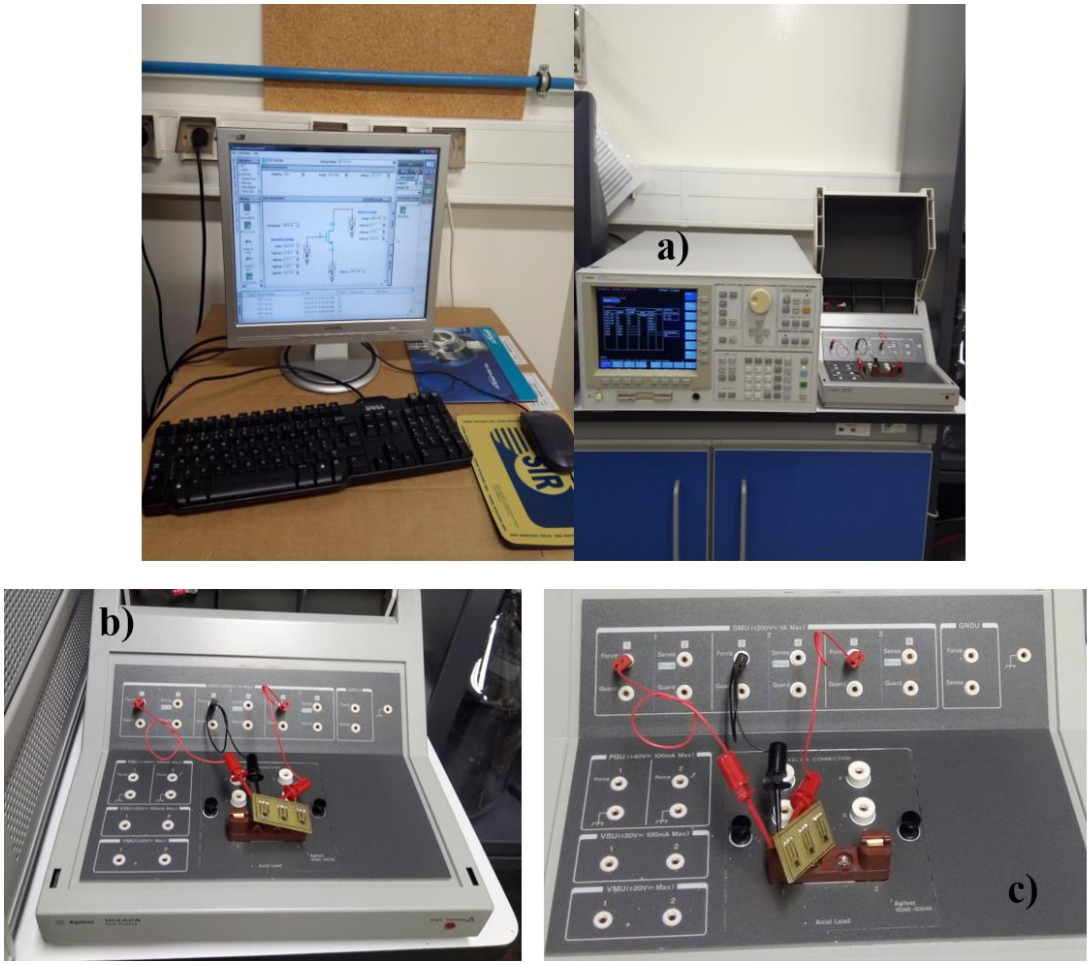

Figure 4 - Apparatuses for the acquisitions of electrical measurements: a) semiconductor parameter analyzer; b) open test fixture with a printed circuit board fixed and drain (D), gate (G) and source (S) of the FET is linked to the respective terminals; c) zoom image of the connection of the FET eletcrode to the text fixture.

For the acquisition of data (drain current (ID) as a function of applied drain voltage (VD)), the software Desktop EasyExpert was used. The electrical signals (ID) were measured at a fixed drain voltage (VD = +1 V) and against a back-gate voltage (VG) of

+1 V, following the steps of graphene deposition, antibody immobilization, and introduction of each sample solution.

3.3 Dispersion of graphene in aqueous solution and spectroscopic characterization

Graphene suspensions of 1 mg mL^{-1} were prepared as follows: 20 mg of graphene nanoplatelets were weighed (#79908, Sigma-Aldrich, Portugal) in a round flask, and 20 mL of aqueous solutions of sodium dodecyl sulphate were prepared (#L6026, Sigma-Aldrich, Portugal) using Mili-Q water. The aqueous solutions of SDS were added to a round bottom flask. After, the graphene suspension was maintained in an ultrasonic water bath (*Branson 2510*), for 60 min at room temperature. During this step, the water bath temperature was monitored in order to ensure that the temperature did not exceed 40ºC, owing to the fact that previous in-house studies showed that this could affect the stability of the suspension. In the end, 9 ml of the suspension in the round bottom flasks were transferred to two 15 mL centrifuge tubes to be centrifuged (*Pro-Research K2015 Ambient Centrifuge*) during 7 min at 2000rpm. The resulting supernatant of each tube were collected for subsequent optical characterization.

For the analysis of the graphene dispersion, ultraviolet-visible spectroscopy (UV–Vis, *Shimadzu UV-2101PC* spectrophotometer) was used. The UV–Vis optical absorbance spectra between 200 and 600 nm was obtained, using a quartz optical cell with 10 cm.

After, for the preparation of Gr-FET, 2 µL of the suspension was deposited on the clean FET surface, allowing it to sit for 15 minutes at room temperature, following a drying step using a N_2 stream.

3.4 Gr-FET for CA 15-3 detection: preparation of anti-CA 15-3 solution, CA 15-3 standard solutions and assessment of analytical performance

Following the drying of the graphene suspension, 2 µL of anti-CA 15-3 solution, diluted in a 1:1000 ratio, prepared from an anti-CA 15-3 solution (*anti-MUC1 antibody*,

antibodiesonline.com) in Dulbecco's phosphate buffered saline solution (PBS, pH 7,4), was dropped on the Gr-FET surface. After, the antibody solution was allowed to dry overnight at 4 °C. Subsequently, a N_2 stream was used to ensure that the antibody solution was completely dried and the output characteristics of the sensor were monitored. The standard solutions of CA 15-3 (0.1, 0.2, 0.5, 1, 2, 3, 4, 5 U mL^{-1}) were prepared in PBS through the dilution of the CA 15-3 protein (*abbexa*) stock solution (50 kU L^{-1}), being this dilution validated by the manufacturer. Then, 2 μL of each solution were deposited onto a minimum of three FET, in order to calculate their reproducibility. After a delay of 15 min, the output characteristics of Gr-FET with CA 15-3 standard solutions were also monitored and for repeatability estimation, two analytical measurements were performed in each Gr-FET. The previously described steps are summarized in Figure 5.

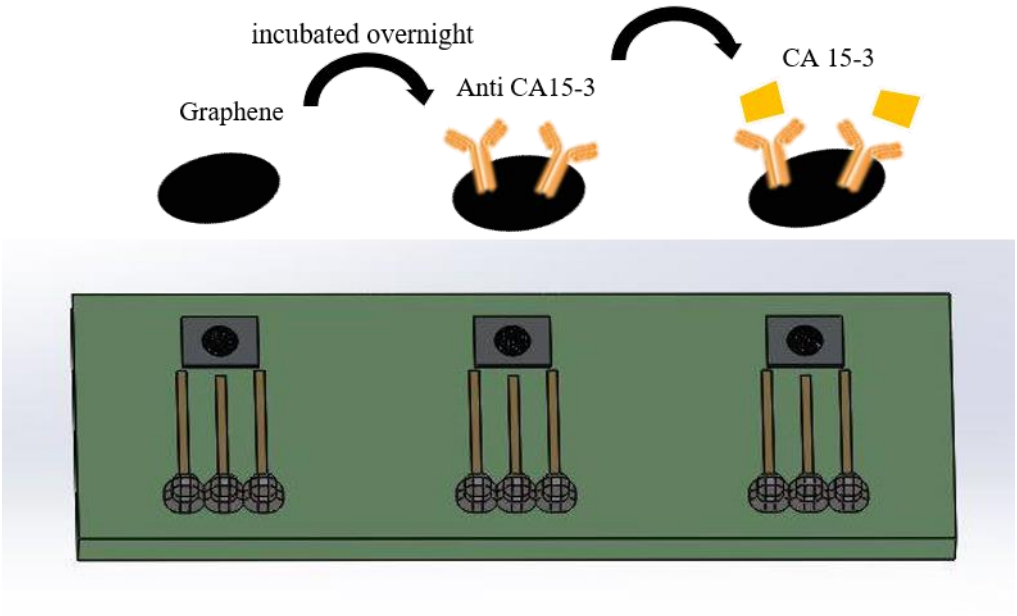

Figure 5 - Schematic representation of the steps followed for the determination of CA 15-3 using Gr-FET.

3.5 Validation of Gr-FET with ELISA

The standard solutions of CA 15-3 were tested with ELISA in order to compare and validate the tested biosensors. A standard ELISA microtiter plate of 96 wells for the determination of CA 15-3 concentrations (containing standards of 10, 50, 150 and 300 U

mL^{-1}) was used, according to the protocol provided by Antibodies.online, that included the following steps, also schematized in Figure 6:

1. 100 µL of standard solutions were added into the wells of the ELISA microtiter plate, in quadruplicates;
2. 100 µL of sample diluent were added into the wells of the ELISA microtiter plate, in quadruplicates, as well 10 µL of sample;
3. Reagents were mixed and incubated in a dark environment for one hour at 37ºC;
4. After incubation, each well was aspirated and washed three times using the washing buffer solution;
5. 100 µL of enzyme conjugate solution was added to the individual wells successively using a multi-channel pipette;
6. The mixture was mixed and incubated for another hour at 37ºC in a dark environment and, after, each well was aspirated and washed three times using the washing buffer solution;
7. 50 µL of the substrate A and 50 µL substrate B were added (to react with the enzyme peroxidase);
8. Reagents were mixed and incubated for 15 min at room temperature;
9. 50 µL of stop solution was added to the wells in the same sequence as for the substrate solution.

After the immunoreaction occurred in the ELISA microtiter plate, the absorbance readings were performed at 450 nm (*SpectraMax PLUS 384*).

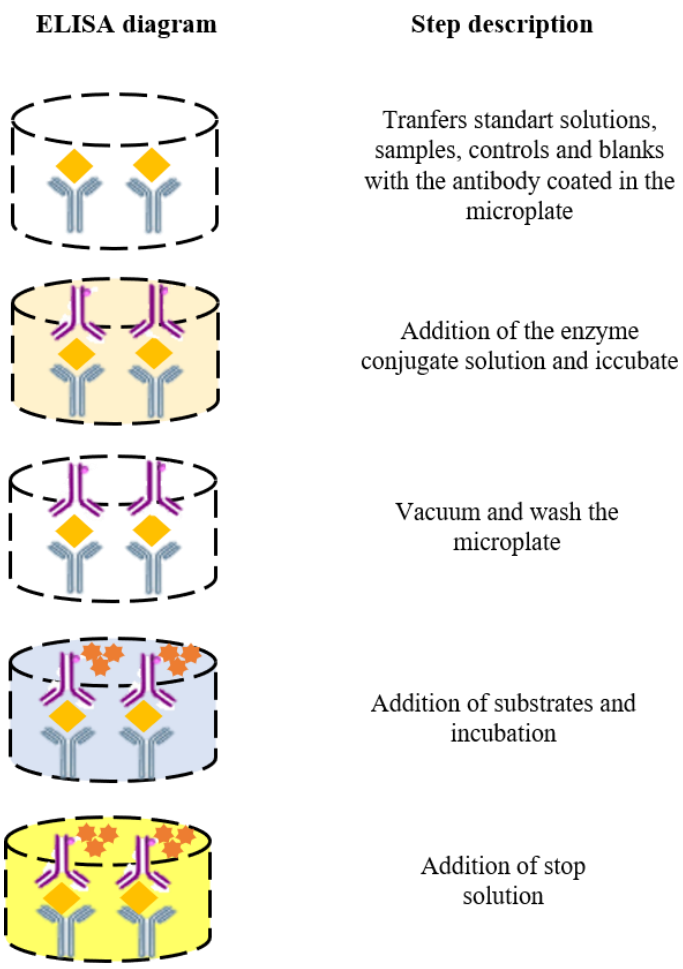

Figure 6 - Schematic of the steps of the ELISA technique.

Finally, the B/B0 values calculated from the standard solutions that were plotted against their respective concentrations were determined and an equation was fitted in order to obtain a calibration model. Also, the B/B0 values calculated from the samples were used for the estimation of the concentration of CA 15-3 in these samples.

3.6 Gr-FET for CA 15-3 detection: preparation of saliva sample solution and analytical performance

For experimental purposes, in order to verify the analytical performance of Gr-FET using biofluids samples, tests were carried out using saliva. Saliva was collected from a single donor after their informed consent. The subject showed good oral health

and hygiene and did not exhibited signs of oral inflammations or other conditions. Additionally, saliva collection took place after a minimum of 30 min after the last meal. This collection was made by passive drooling into a centrifugation tube, kept in ice, until a workable volume (approximately 7.5 mL) was obtained. After, the samples were stored at 4ºC until further use.

Spiked solutions of CA 15-3 (2, 2.5, 3, 4 U mL^{-1}) in saliva were prepared through dilution of the CA 15-3 stock solution (50 kU L^{-1}), that is validated by the manufacturer and is also used for the ELISA technique. As mentioned above, saliva solution containing the analyte was placed (2 μL) on the FET surface following the functionalization of graphene with anti-CA 15-3. After, the output characteristics were monitored. Again, two analytical measurements were performed in each Gr-FET for the repeatability estimation. Recoveries were determined based on the calibration curve obtained for the tested Gr-FET biosensor.

4. Results and Discussion

4.1 Dispersion of graphene in SDS by spectroscopic characterization

Following the preparation steps described in section 3.3, the final graphene suspensions prepared showed a homogenous dark colour, as evidenced in Figure 7.

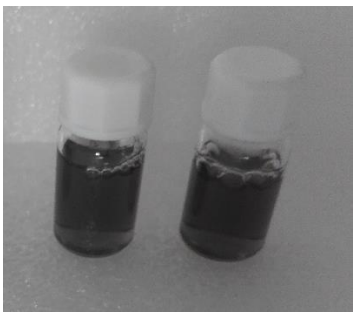

Figure 7 - Dispersion of graphene, after a sonication and followed by a centrifugation.

The homogeneity of the solution observe in the figure 7, results from the use of the ultrasounds bath, whose mechanical energy allows for the disaggregation of the graphene, by balancing the van der Walls forces.[39],[40] The subsequent centrifugation steps allows for the separation the graphene from the amorphous carbon and graphite from the previous step before.[38]

The absorbance spectra, shown in Figure 8, highlight the presence of a slight interband from electronic transition of the graphene in the region of 228 nm. This may be attributable to the π-π^* transitions of the aromatic C-C bonds[41]. In order to assess the temporal stability of the prepared graphene suspensions, UV-Vis spectra of these suspensions were also obtained for a period of 14 days. As shown in Figure 8, spectroscopic characterization evidences the similarities in the obtained spectra, highlighting the stability of these suspensions.

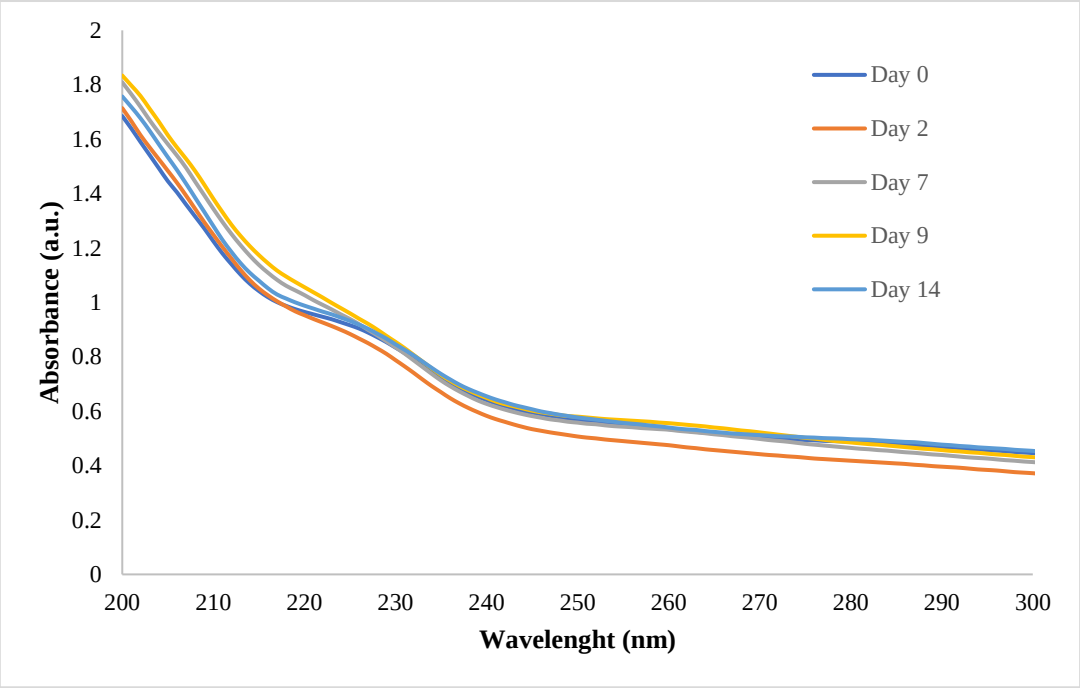

Figure 8 - Absorbance spectra of the dispersion of graphene in SDS after day 0, 2, 7, 9 and 14.

4.2 Analytical performance of Gr-FET for CA 15-3 detection

In figure 9, the analytical response of the Gr-FET after each step is shown. The results, describing the variation of the output current (I_D) in function of the drain voltage (V_D), demonstrate the linear relationship I_D-V_D, implying an effective transport of electrons on the graphene layers[42], following the initial graphene deposition. After the anti-CA 15-3 immobilization, the measured current decreases, likely due to the supply of electrons to the graphene film by the antibody, decreasing the number of available holes and, consequently, decreasing the drainage current[43].

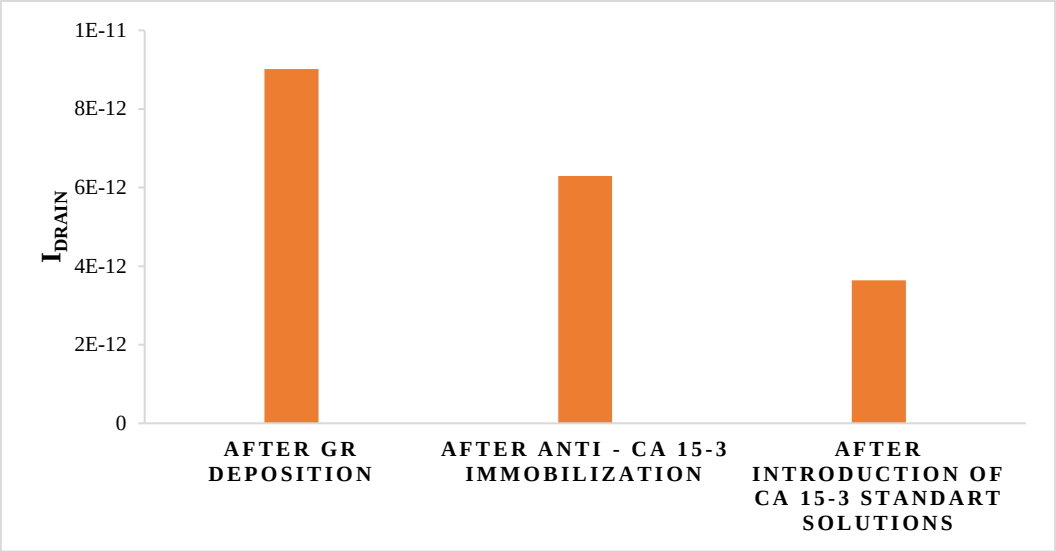

Figure 9 - Output characteristics obtained after deposition of Gr-FER, after immobilization of anti-CA 15-3 and after introduction of CA 15-3 standard solutions.

Lastly, there is also a reduction on the measured current after the addition of the analyte, in this case, CA 15-3. This probably stems from the fact that this is a non-ionic molecule, thus preventing electroactive species from entering the film in order to contact the electrode. This, in turn, reduces the exchange of electrons between the electrode and the molecules[44]. This phenomenon was also noticeable with increasing concentrations of CA 15-3, effectively demonstrating that this molecule induces a *de facto* kinetic barrier for electron transfer, thus decreasing the I_D[45]. That is, the greater the concentration of the standard solution, the greater will be the binding on the antibody and greater the degree of immobilization, which creates an insulating layer on the electrode surface through adsorption, making electron transfer difficult[44].

Figure 10 shows the log-log calibration curve obtained with the CA 15-3 standard solutions. The method clearly indicates a linear relationship between the logarithm of the analytical response of CA 15-3 against logarithm of CA 15-3 concentrations with the following regression equation:

(Eq. 1) $y = 0{,}6965\,x - 11{,}415$

where y is the output current and x (in XA) the concentration of CA 15-3 (in U mL^{-1}). The statistically difference determined ($p < 0{,}001$) between the several CA 15-3 concentrations means that the Gr-FET has markedly different responses depending on the CA 15-3 concentration. The determined coefficients of variation ((standard

deviation/average) x100%) determined for each reading varied from 0.99% to 2.23% for the tested concentrations. The calculated average CV of 2.12 ± 0.65 % highlights the good repeatability and an adequate reproducibility of the developed Gr-FET. The concentration of 0.07 U ml^{-1} was considered as the limit of detection (LoD), as the minimum detectable concentration. Since the calibration curve stems from a log-log correlation, the limit of detection could not be mathematically determined through the traditional method ($y_{LOD} = y_B + 3S_B$, where y_{LOD} is the signal, y_B is the mean of the signal from the blank sample and s_B is the standard deviation of the intercepts of the derivation from the blank sample)[46], as *x* tends to approximate zero and *y* tends to infinite.

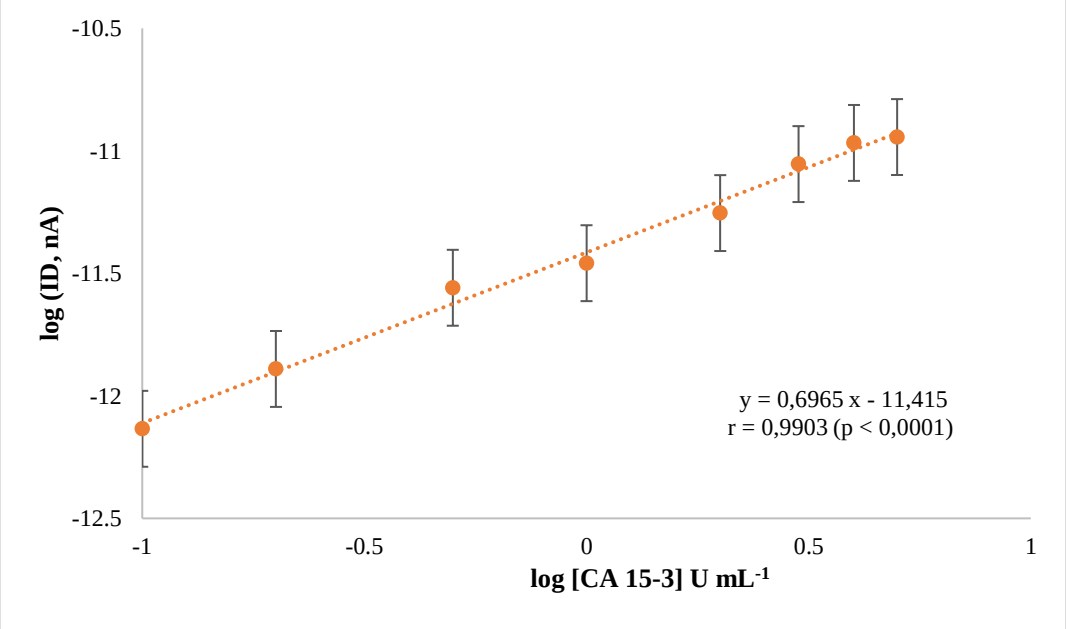

Figure 10 - Log-log regression plot for the analytical response of Gr-FET to CA 15-3 standard solutions.

The limit of detection found for the herein developed Gr-FET (0.07 U mL^{-1}), that was mathematically estimated, is considerably lower than other reported for the detection and quantification of CA 15-3. Other sensors, resorting to materials such as nano-dots or gold nanoparticles, have been described as showing LoD ranging from 0.9 U mL^{-1} to 5 U mL^{-1} [33,47–50].

4.3 Recovery analysis of standard samples by Gr-FET

To evaluate the recovery of CA 15-3 and, simultaneously, the Gr-FET performance, recovery assays were conducted. These consisted in assessing the electrical performance of the Gr-FET when using solutions containing known concentrations of the analyte and then calculating the estimated concentrations from the electrical signals measured. For this, different concentrations from the established standard were used (1.20, 1.40, 2.50 and 3.50 U mL^{-1}).

Table 2 shows that the concentration found values were very close to those theoretically present in the solutions. In fact, the range of the recoveries obtained varied between 97-101 %, with an average of 99.10 %. These results suggest that the Gr-FET exhibits excellent performance and a good recovery of CA 15-3.

Table 2 - Recovery of CA 15-3 obtained in standard samples in Gr-FET.

Standard Samples		
[CA 15-3] (U mL^{-1})	**Found concentration (U mL^{-1})**	**Mean recovery ± SD (%)**
1.20	1.21	100.8 ± 6.67
1.40	1.36	97.1 ± 3.47
2.50	2.51	100.4 ± 0.12
3.50	3.43	98.0 ± 1.06

4.4 Recovery analysis in saliva samples

In order to assess the applicability of the developed biosensor for the detection and quantification of CA 15-3 in saliva samples, thus potentially significantly decreasing time and cost of analysis, as well as establishing an effective non-invasive method for said quantification, recovery of CA 15-3 in saliva samples was conducted, resorting to

spiked solutions containing 2.0, 2.50, 3.0, and 4.0 U mL $^{-1}$. The experimental results are shown in Table 3.

Table 3 - Comparison of the recovery of CA 15-3 obtained in standard samples and saliva samples in Gr-FET.

	Standard Samples		**Saliva Samples**	
[CA 15-3] (U mL^{-1})	**Found concentration (U mL^{-1})**	**Mean recovery ± SD (%)**	**Found concentration (U mL^{-1})**	**Mean recovery ± SD (%)**
2.0	1.97	98.5 ± 1.61	2.32	116.0 ± 1.09
2.50	2.51	100.4 ± 0.12	2.56	102.4 ± 2.95
3.0	3.01	100.3 ± 2.24	2.99	99.6 ± 2.18
4.0	4.03	100.7 ±0.93	4.44	111.0 ± 1.49

Table 3 shows the values obtained for the recovery of CA 15-3 in samples with different solutions and that the concentration found is very close to the value of CA 15-3. For the standard samples it was obtained a recovery of 98.50 %, 100.40 %, 100.33 % and 100.75 % with an average of 99.99 %. For the saliva samples it was obtained a recovery of 116.00 %, 102.40 %, 99.66 % and 111.00 % with an average of 107.26 %. The range obtained for both samples was between 98-116 %, and being the aceptable range between 98 – 102 % , besides the value exceeds a narrowly the ideal value and considering the number of concentrations used is acceptable. This way, these results reveal the accuracy of the Gr-FET in different samples a good recovery of CA 15-3.

4.5 Analytical performance of ELISA and Gr-FET techniques for CA 15-3

The ELISA method was used to validate the results obtained using the Gr-FET. The mathematically determined correlation between the CA 15-3 concentration and

absorbance at 450 nm is shown in Figure 11. The shown inset pertains to the original data obtained.

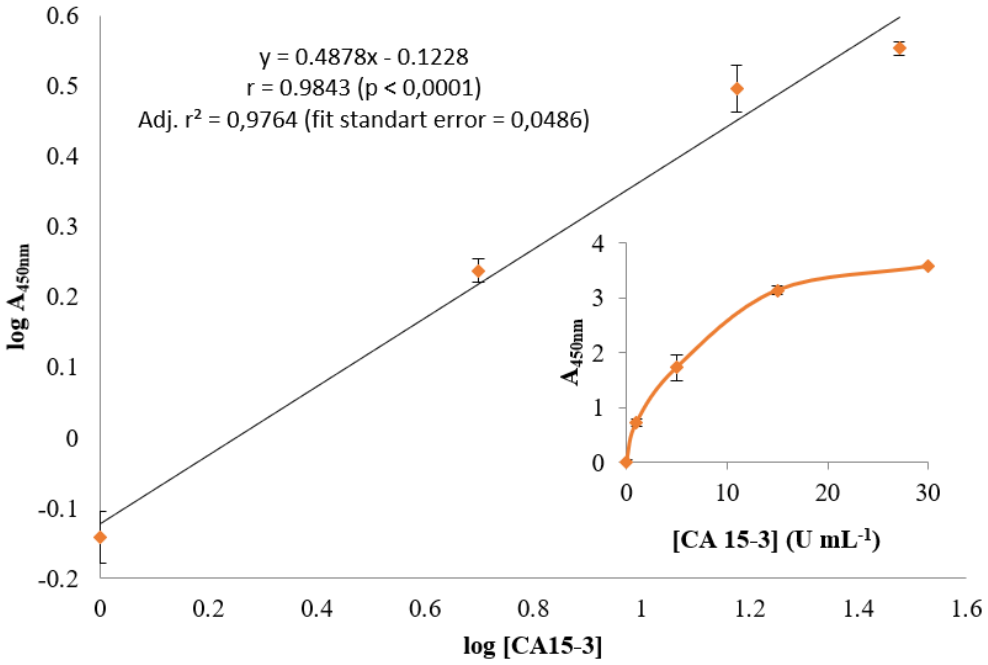

Figure 11 – Log-log regression plot for the analytical response of ELISA to CA 15-3 standard solutions, with an inset of the absorbance spectra for [CA 15-3].

Subsequently, in order to validate the data obtained using the developed biosensor, the recovery of CA 15-3 samples, through ELISA and Gr-FET techniques, was assessed. For this purpose, concentrations of CA 15-3 of ranging from 4 to 7.5 $U.mL^{-1}$ were used. Extrapolation was performed to verify values for concentrations greater than 5, and the values were not too high to apply to the calibration line.

In Table 4, the recovery ranges determined are shown. These varied from 99.07 to 110.09 for ELISA and a ranged from 97.86 to 101.6 % for Gr-FET. For ELISA and Gr-FET, average recoveries were 105.9 % and 99.8 % for Gr-FET, respectively.

Table 4 - Recovery of CA 15-3 obtained for ELISA and Gr-FET in samples.

	Gr-FET		ELISA	
[CA 15-3] (U mL^{-1})	**Found concentration (U mL^{-1})**	**Mean recovery ± SD (%)**	**Found concentration (U mL^{-1})**	**Mean recovery ± SD (%)**
4.50	4.57	101.6 ± 0.58	4.99	110.9 ± 0.76
5.0	5.07	101.4 ± 2.71	5.53	110.6 ± 1.91
6.0	5.93	98.3 ± 0.67	6.18	103.0 ± 2.76
7.50	7.34	97.9 ± 3.27	7.43	99.07 ± 1.17

The CA 15-3 concentrations obtained through the two methods appeared to agree to a satisfactory level, as evidenced in Table 4. As such, and considering the described steps involved in the use of the ELISA method, it becomes apparent that the herein developed technology provides similar results in a pointedly less time-consuming method, thus paving the way for future applications in POC settings.

5. Conclusions

In this work, a disposable – yet re-usable – FET sensor for the detection and quantification of CA 15-3, based on graphene as transduction component, was developed.

The biosensor was shown to be able to quantify CA 15-3 within a linear range between 0.1 and 5 U mL^{-1}, while displaying a limit of detection of 0.07 U mL^{-1}.

Furthermore, the developed biosensor was evaluated as a non-invasive tool for the quantification of this protein, currently used as a biomarker for breast cancer, in saliva samples.

More broadly, these results have evidenced the potential application of Gr-FET in the area of clinical diagnosis, and the potential time, cost and efficacy gains when compared to more traditionally used techniques. The herein described work also highlights the potential of biosensors, in general, and of electrochemical biosensors, in particular, to be used as Point-Of-Care devices, thus allowing instantly obtaining and sharing the clinically relevant data with care providers.

Results showed that such use is possible, although further validation, including the use of a more extensive array of subjects, patients known to have elevated values of CA 15-3, is necessary. Furthermore, the field of application of the developed Gr-FET should also be tested in other bodily fluids, such as urine, in order to expand the potential use of this technology in the diagnosis, treatment and monitoring of cancer patients.

References

1. Balaji, A. & Zhang, J. Electrochemical and optical biosensors for early-stage cancer diagnosis by using graphene and graphene oxide. *Cancer Nanotechnol.* **8**, (2017).

2. Begum, M. *et al.* CA 15-3 (Mucin-1) and Physiological Characteristics of Breast Cancer from Lahore , Pakistan. *Asian Pacific J. Cancer Prev.* **13**, 5257–5261 (2012).

3. Campuzano, S., María, P. & Pingarrón, J. M. Non-Invasive Breast Cancer Diagnosis through Electrochemical Biosensing at Different Molecular Levels. *Sensors* (2017). doi:10.3390/s17091993

4. Tumor Markers. Available at: https://www.cancer.gov/about-cancer/diagnosis-staging/diagnosis/tumor-markers-fact-sheet. (Accessed: 17th October 2019)

5. Safi, F. & MD, I. K. The Value of the Tumor Marker CA 15-3 in Diagnosing and Monitoring Breast Cancer A comparative Study With Carcinoembryonic Antigen. *Cancer* (1990).

6. Duffy, M. J. *et al.* High Preoperative CA 15-3 Concentrations Predict Adverse Outcome in Node-Negative and Node-Positive Breast Cancer : Study of 600 Patients with Histologically Confirmed Breast Cancer. *Clin. Chem.* **563**, 559–563 (2004).

7. Heiligtag, F. J. & Niederberger, M. The fascinating world of nanoparticle research. *Mater. Today* **16**, 262–271 (2013).

8. Agha-hosseini, F., Mirzaii-dizgah, I. & Rahimi, A. Correlation of serum and salivary CA15-3 levels in patients with breast cancer. **14**, 521–524 (2009).

9. Shao, Y., Sun, X., He, Y., Liu, C. & Liu, H. Elevated Levels of Serum Tumor Markers CEA and CA15-3 Are Prognostic Parameters for Different Molecular Subtypes of Breast Cancer. *PLoS One* 1–11 (2015). doi:10.1371/journal.pone.0133830

10. Farzin, L. & Shamsipur, M. Recent advances in design of electrochemical

affinity biosensors for low level detection of cancer protein biomarkers using nanomaterial-assisted signal enhancement strategies. *J. Pharm. Biomed. Anal.* (2017). doi:10.1016/j.jpba.2017.07.042

11. Mittal, S., Kaur, H., Gautam, N. & Mantha, A. K. Biosensors for breast cancer diagnosis: A review of bioreceptors, biotransducers and signal amplification strategies. *Biosens. Bioelectron.* **88**, 217–231 (2017).

12. Ranjan, R., Esimbekova, E. N. & Kratasyuk, V. A. Rapid biosensing tools for cancer biomarkers. *Biosens. Bioelectron.* **87**, 918–930 (2017).

13. Justino, C. I. L., Rocha-santos, T. A. & Duarte, A. C. Review of analytical figures of merit of sensors and biosensors in clinical applications. *Trends Anal. Chem.* **29**, 1172–1183 (2010).

14. Picó, Y. *Chemical Analysis of Food: Techniques and Applications*. (2012).

15. Electrochemical Biosensors - an overview. Available at: https://www.sciencedirect.com/topics/engineering/electrochemical-biosensors. (Accessed: 17th October 2019)

16. Pohanka, M. & Skladal, P. Electrochemical Biosensors-Principles and Applications. (2008). doi:10.32725/jab.2008.008

17. Grieshaber, D., MacKenzie, R., Voros, J. & Reimhult, E. Electrochemical Biosensors - Sensor Principles and Architectures. *Sensors* 1400–1458 (2008).

18. Stradiotto, N. R., Yamanaka, H. & Zanoni, M. V. B. Review Electrochemical Sensors : A Powerful Tool in Analytical Chemistry. *J. Braz. Chem. Soc* **14**, 159–173 (2003).

19. Marques, I. *et al.* Carbon nanotube field effect transistor biosensor for the detection of toxins in seawater. *Int. J. Environ. Anal. Chem.* **00**, 1–9 (2017).

20. Rhiannan, F., Anitha, D. & Guy J., O. Graphene Field Effect Transistors for Biomedical Applications : Current Status and Future Prospects. *Diagnostics* (2017). doi:10.3390/diagnostics7030045

21. Anju, M. & Renuka, N. K. Graphene – dye hybrid optical sensors. *Nano-Structures & Nano-Objects* **17**, 194–217 (2019).

22. Zhu, Z. An Overview of Carbon Nanotubes and Graphene for Biosensing Applications. *Nano-Micro Lett.* **9**, 1–24 (2017).

23. Byrne, B., Stack, E., Gilmartin, N. & Kennedy, R. O. Antibody-Based Sensors: Principles, Problems and Potential for Detection of Pathogens and Associated Toxins. *Sensors* 4407–4445 (2009). doi:10.3390/s90604407

24. Sharma, S., Byrne, H. & Kennedy, R. J. O. Antibodies and antibody-derived analytical biosensors. *Essays Biochem.* 9–18 (2016). doi:10.1042/EBC20150002

25. Sharma, S., Byrne, H. & Kennedy, R. J. O. Antibodies and antibody-derived analytical biosensors. 9–18 (2016). doi:10.1042/EBC20150002

26. Li, W., Yuan, R., Chai, Y. & Chen, S. Reagentless amperometric cancer antigen 15-3 immunosensor based on enzyme-mediated direct electrochemistry. *Biosens. Bioelectron.* **25**, 2548–2552 (2010).

27. Li, H., He, J., Li, S. & Turner, A. P. F. Electrochemical immunosensor with N -doped graphene-modified electrode for label-free detection of the breast cancer biomarker CA 15-3. *Biosens. Bioelectron.* **43**, 25–29 (2013).

28. Marques, R. C. B. *et al.* Voltammetric immunosensor for the simultaneous analysis of the breast cancer biomarkers CA 15-3 and HER2-ECD. *Sensors and Actuators* **255**, 918–925 (2017).

29. Amani, J., Khoshroo, A. & Rahimi-nasrabadi, M. Electrochemical immunosensor for the breast cancer marker CA 15 – 3 based on the catalytic activity of a CuS / reduced graphene oxide nanocomposite towards the electrooxidation of catechol. *Springer Nat.* **2**, 1–9 (2017).

30. Akbari, S., Khalilzadeh, B., Samadi, P. & Saber, R. A highly sensitive and reliable detection of CA15-3 in patient plasma with electrochemical biosensor labeled with magnetic beads. *Biosens. Bioelectron.* **122**, 8–15 (2018).

31. Nguyen, H. L., Nguyen, D. T., Do, Q. P. & Tran, L. D. Electrosynthesized

poly(1,5-diaminonaphthalene)/polypyrrole nanowires bilayer as an immunosensor platform for breast cancer biomarker CA 15-3. *Curr. Appl. Phys.* **17**, 1422–1429 (2017).

32. Hasanzadeh, M., Tagi, S., Solhi, E. & Shadjou, N. Immunosensing of breast cancer prognostic marker in adenocarcinoma cell lysates and unprocessed human plasma samples using gold nanostructure coated on organic substrate. *Int. J. Biol. Macromol.* **118**, 1082–1089 (2018).

33. Ribeiro, J. A., Pereira, C. M., Silva, A. F. & Sales, M. G. F. Disposable electrochemical detection of breast cancer tumour marker CA 15- 3 using poly (Toluidine Blue) as imprinted polymer receptor. *Biosens. Bioelectron.* **109**, 246–254 (2018).

34. Wang, X., Yu, H., Lu, D., Zhang, J. & Deng, W. Label free detection of the breast cancer biomarker CA15 . 3 using ZnO nanorods coated quartz crystal microbalance. *Sensors Actuators B. Chem.* **195**, 630–634 (2014).

35. Mohammadi, S., Salimi, A., Hamd-ghadareh, S. & Fathi, F. A FRET immunosensor for sensitive detection of CA 15-3 tumor marker in human serum sample and breast cancer cells using antibody functionalized luminescent carbon-dots and AuNPs-dendrimer aptamer as donor-acceptor pair. *Anal. Biochem.* **557**, 18–26 (2018).

36. Marques, I. *et al.* Carbon nanotube field effect transistor biosensor for the detection of toxins in seawater. *Int. J. Environ. Anal. Chem.* **97**, 597–605 (2017).

37. Antunes, J. *et al.* Graphene immunosensors for okadaic acid detection in seawater. *Microchem. J.* **138**, 465–471 (2018).

38. Justino, C. Nanosensor for assenssing the risk of a cardiovascular disease. *Thesis Univ. Aveiro* (2013).

39. Taylor, P., Hilding, J., Grulke, E. A., Zhang, Z. G. & Lockwood, F. Dispersion of Carbon Nanotubes in Liquids. *J. Dispers. Sci. Technol.* 37–41 (2007).

40. Vaisman, L., Wagner, H. D. & Marom, G. The role of surfactants in dispersion of

carbon nanotubes. *Adv. Colloid Interface Sci.* **130**, 37–46 (2007).

41. Kuila, T., Bose, S., Kumar, A. & Khanra, P. Chemical functionalization of graphene and its applications. *Prog. Mater. Sci.* **57**, 1061–1105 (2012).

42. Ma, X., Gu, W., Shen, J. & Tang, Y. Investigation of electronic properties of graphene / Si field-effect transistor. *Nanoscale Res. Lett.* **7**, 1 (2012).

43. Justino, C. Nanosensor for assenssing the risk of a cardiovascular disease. *Thesis Univ. Aveiro* (2013).

44. Bollella, P., Fusco, G., Tortolini, C., Sanzò, G. & Favero, G. Beyond graphene : Electrochemical sensors and biosensors for biomarkers detection. *Biosens. Bioelectron.* **89**, 152–166 (2017).

45. He, Q., Yin, Z. & Zhang, H. Graphene-based electronic sensors. *Chem. Sci.* (2012). doi:10.1039/C2SC20205K

46. Miller, J. N. & Miller, J. C. *Statistics and Chemometrics for Analytical Chemistry*.

47. Mohammadi, S., Salimi, A., Hamd-ghadareh, S. & Fathi, F. A FRET immunosensor for sensitive detection of CA 15-3 tumor marker in human serum sample and breast cancer cells using antibody functionalized luminescent carbon-dots and AuNPs-dendrimer aptamer as donor-acceptor pair. *Anal. Biochem.* **557**, 18–26 (2018).

48. Hasanzadeh, M., Tagi, S., Solhi, E., Mokhtarzadeh, A. & Shadjou, N. An innovative immunosensor for ultrasensitive detection of breast cancer speci fi c carbohydrate (CA 15-3) in unprocessed human plasma and MCF-7 breast cancer cell lysates using gold nanospear electrochemically assembled onto thiolated graphene quantum . *Int. J. Biol. Macromol.* **114**, 1008–1017 (2018).

49. Marques, R. C. B. *et al.* Voltammetric immunosensor for the simultaneous analysis of the breast cancer biomarkers CA 15-3 and HER2-ECD. *Sensors Actuators B Chem.* **255**, 918–925 (2018).

50. Pacheco, J. G., Silva, M. S. V, Freitas, M., Nouws, H. P. A. & Delerue-matos, C.

Molecularly imprinted electrochemical sensor for the point-of-care detection of a breast cancer biomarker (CA 15-3). *Sensors Actuators B. Chem.* **256**, 905–912 (2018).